Heliyon

Received:
8 November 2018
Revised:
22 January 2019
Accepted:
20 February 2019

Cite as: Jagmit Singh, Luis E. Zerpa, Benjamin Partington, Jose Gamboa. Effect of nozzle geometry on critical-subcritical flow transitions. Heliyon 5 (2019) e01273. doi: 10.1016/j.heliyon.2019.e01273

Effect of nozzle geometry on critical-subcritical flow transitions

Jagmit Singh [a], **Luis E. Zerpa** [a,*], **Benjamin Partington** [b], **Jose Gamboa** [b]

[a] *Department of Petroleum Engineering, Colorado School of Mines, 1500 Illinois St., Golden, CO 80401, USA*

[b] *Chevron ETC, Houston, TX, USA*

[*] Corresponding author.

E-mail address: lzerpa@mines.edu (L.E. Zerpa).

Abstract

The geometry of converging-diverging nozzles affects the conditions at which critical-subcritical flow transition occurs. The objective of this work is to develop guidelines to identify the optimum nozzle geometry that maximizes critical pressure ratio while minimizing pressure drop across the nozzle. Experiments were conducted in a facility with 1.5 in. ID PVC pipelines and a 30 ft. long lateral pipeline section. In total, 27 different nozzle geometries were tested, divided into two groups − conical and parabolic nozzles. Nozzles from the ASTAR, Deich, LJ and Moby Dick nozzle groups showed improved performance compared to other nozzle groups. It was determined that a smaller diverging angle and absence of an elongated throat resulted in a higher critical pressure ratio. Length of converging and diverging sections of nozzles did not have as much of an impact on nozzle performance as the throat diameter and shape of converging and diverging sections.

Keyword: Mechanical engineering

1. Introduction

A nozzle is a venturi device that, given sufficient upstream pressure and flow conditions, can result in choked flow at its throat. Nozzles are used in different industries

https://doi.org/10.1016/j.heliyon.2019.e01273

for different purposes such as to accelerate flow for atomization of liquid phases, as part of jets to increase kinetic energy and to propel gas in rocket engines, in natural gas production wells to accelerate gas velocity, among many others. The nozzle geometry plays a very important role to achieve choked flow conditions. In most applications, it is important to optimize the nozzle design to minimize pressure drop due to increased velocities at the nozzle throat.

Nozzles have three different sections – converging section, throat and diverging section, as shown in Fig. 1. The point where the diameter of the nozzle is the smallest is called the throat. The throat can either be a single point or it can be elongated. The section upstream of the throat is the converging section, and the section downstream of throat is the diverging section. The area of the converging section decreases as the nozzle profile goes from pipe to the beginning of the throat. The area of diverging section increases as the nozzle profile goes from the end of the throat to the pipe.

The fluid flow behavior through nozzles also depends on the type of fluid flowing through the nozzle. The dimensionless Mach number, M, which is the ratio of fluid velocity to velocity of sound in the surrounding medium, can be calculated to determine if the flow is compressible ($M > 0.2$) or incompressible ($M < 0.2$). In this work, compressible flow is considered by using air as working fluid. Flow velocity increases as fluid enters the nozzle, until the nozzle throat is reached. At this point flow is subsonic (i.e. $M < 1$). Once fluid flows through the throat, given sufficient upstream pressure and flowrate conditions, the fluid velocity could become equal to the velocity of sound, reaching sonic conditions (i.e. $M = 1$). As fluid flows out of the throat, entering the diverging section, the fluid velocity increases beyond the speed of sound reaching supersonic flow (i.e. $M > 1$). This occurs because when air is flowing through the diverging section of the nozzle, there is an increase in kinetic energy at the expense of an enthalpy drop due to gas expansion.

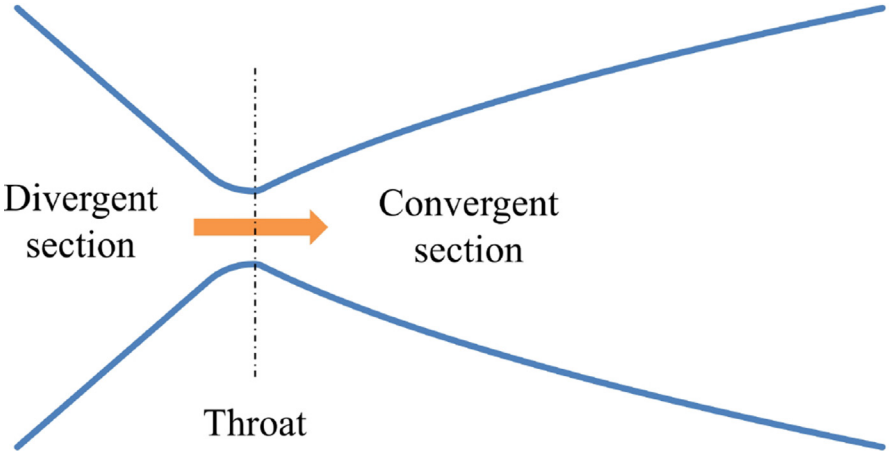

Fig. 1. Schematic of a converging-diverging nozzle indicating the different sections of a typical nozzle (Clarke and Carswell, 2007).

https://doi.org/10.1016/j.heliyon.2019.e01273

The purpose of using a nozzle is to accelerate the flow to achieve critical or sonic conditions (i.e., choked flow) at its throat. This happens as the pressure differential upstream and downstream the nozzle increases. At a certain pressure differential, the flowrate through the nozzle for that particular throat size reaches a maximum and the Mach number becomes 1. Any further increase in pressure differential does not result in an increase in flowrate. Beyond the point where flowrate stops increasing, the flow is said to be choked. Once this happens, any perturbation that occurs downstream to the throat, in terms of pressure changes, would not affect the upstream flow.

The performance of a nozzle is quantified based on critical pressure ratio and pressure drop across the nozzle. Critical pressure ratio is the lowest ratio of downstream pressure to upstream pressure (P_d/P_u) when the flow is choked. Below this pressure ratio, the flow is sub-critical. An optimum nozzle geometry is one where choked flow is achieved at a larger critical pressure ratio value when compared to other nozzle geometries. This is associated with a higher pressure recovery as the fluid exits the throat of the nozzle and travels through the divergent section, minimizing pressure drop across the nozzle.

This work studies the effects of geometrical parameters such as shape of converging and diverging section, throat length, and nozzle diverging and converging angle on the performance of nozzles. Previous studies conducted focus on evaluating nozzle performance by varying some of the above-mentioned parameters. Almeida (2015) investigated the effect of nozzle parameters (diverging angle, throat length and shape of diverging section) on nozzle performance. The basic design of the nozzle studied included a convex converging section and a linear diverging section. This work concluded that a higher diverging angle, larger throat length and the shape of the diffuser section have significant and detrimental impact on nozzle performance (Almeida, 2015). Park et al. (2001), performed a study that also showed that higher diverging angles resulted in lowered nozzle performance. The considered nozzle shape had a convex converging section and a linear diverging section. Conclusions drawn from this study are in line with the conclusions reached in this paper (Park et al., 2001).

In both studies mentioned above, the nozzle shape remained the same. No other shapes were tested to determine if others would increase nozzle performance. The objective of this work is to conduct experimental analysis on different nozzle geometries and determine the effect of geometrical parameters and shapes on nozzle performance. Additionally, the optimal nozzle design is identified based on the experimental data collected. An optimal nozzle design is one that maximizes the critical pressure ratio whilst minimizing the pressure drop across the nozzle.

2. Design

In order to create a matrix of different nozzle geometries and shapes, we conducted a review of nozzles implemented in industries such as aerospace, agricultural, nuclear

https://doi.org/10.1016/j.heliyon.2019.e01273

and petroleum. Based on this research, nozzles can be classified into two main shapes: conical and parabolic.

A conical nozzle, or a converging-diverging nozzle, has a downward tapering linear inlet area which reduces in cross-sectional area along the profile until the throat diameter has been reached, and then has an upward tapering linear outlet area where the cross-sectional area increases along the profile (Fig. 2). The angle at which the inlet tapers is called converging angle (β). The angle at which the outlet tapers is called the diverging half angle (α). The diameter of the smallest point in the nozzle is called the throat diameter (D_t).

The cone half angle should not exceed 15°, to avoid nozzle internal flow losses (Östlund, 2002). According to Barber, the value of cone divergence half angle should be between 2 and 12° (Barber and Schultheiss, 1967). Limited studies provide a definitive value or range of the converging angle, but generally it is about 45°. Varying the converging angle possibly does not have as much effect as the diverging half angle, because the flow is still sub-sonic in the converging region of the nozzle. However, a different shape of the converging section may have an impact on the pressure drop across the nozzle.

Based on these considerations, three different conical nozzle configurations are considered in this study:

1. **Converging − Diverging Nozzle:** This is a basic de Laval nozzle without an elongated throat that is used in many applications such as steam turbines and rocket engines.
2. **Modified Converging − Diverging Nozzle:** The design of this nozzle includes an elongated throat length. In the technical report 'Acceleration of liquids in two phase nozzles' by NASA, it was determined that the throat length had an impact on the performance of the nozzle (Elliot and Weinber, 1968).

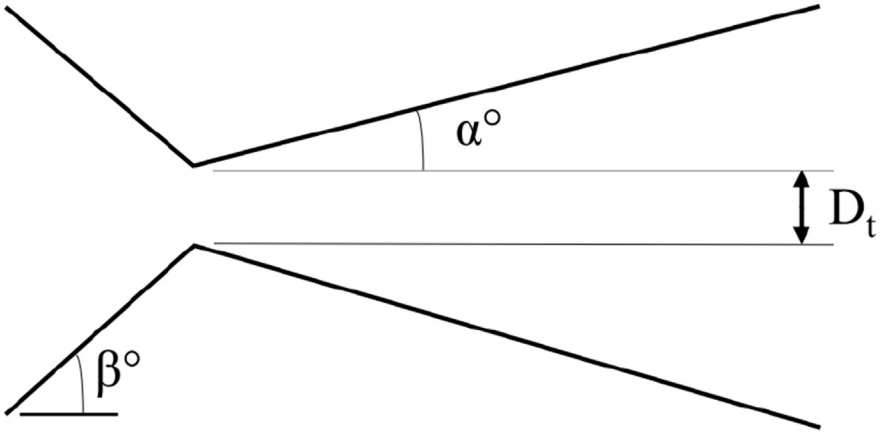

Fig. 2. Basic conical nozzle design features and variables (Modified from Sutton and Biblarz, 2001).

https://doi.org/10.1016/j.heliyon.2019.e01273

3. **Dual Converging Nozzle:** The design for a dual converging nozzle was obtained from a patent of a liquid gas injector in the industry of jet technology (Popov, 2002). It has two subsequent converging sections with decreasing converging angle.

A parabolic nozzle (based on the Rao nozzle shape) has a circular converging section and a parabolic diverging section (Fig. 3). The point from which the parabolic diverging section begins is called nozzle angle (θ_n). The angle created at the end of the nozzle is termed as nozzle exit (θ_e). The radius of the circular converging section is 1.5 times the throat radius. This region continues until the throat is reached. Once the profile of the throat ends, another circle of radius 0.382 times the throat radius is designed. The slope of the parabolic curve is tangent to the inflection point (θ_n), where the divergent curve and the parabolic curve intersect (Kulhanek, 2012). Then at a certain point, a parabola of bell shape is created which constitutes the majority of the diverging section.

This experimental study considers the following eight designs for parabolic shape:

1. **Rao Nozzle:** Rao nozzle is widely used in the aerospace industry to release the exhaust coming from the gas chamber. The main reason to create this nozzle was to get a higher performance nozzle for a shorter length. It is generally about 80% the length of a de Laval nozzle.
2. **Modified Rao Nozzle**: This is a Rao nozzle modified to incorporate an elongated throat to observe the effect of throat length.
3. **Dual Bell Nozzle:** The dual bell nozzle was developed by the aerospace industry to make their rockets more efficient in high altitude conditions. But since in this project the altitude of the nozzle will not be changing, this nozzle would only be tested to note the effect of using this contour on fluid flow. This type of nozzle has two parabolic diverging sections instead of one found on a Rao nozzle (Nürnberger-Genin and Stark, 2009).

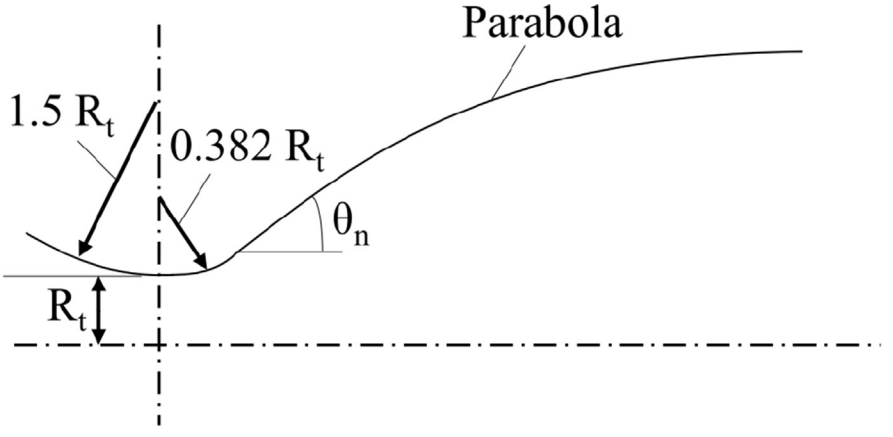

Fig. 3. Basic design and variables for a parabolic nozzle (Modified from Raiano, 2013).

https://doi.org/10.1016/j.heliyon.2019.e01273

4. **Converging Convex Nozzle:** The design for converging convex nozzle was obtained from a patent of a liquid gas injector in the industry of jet technology. This nozzle has a convex circular converging section (Popov, 2002).
5. **Converging Concave Nozzle:** The design for converging concave nozzle was obtained from a patent of a liquid gas injector in the industry of jet technology. This nozzle has a concave circular converging section that extends all the way to the entrance radius (Popov, 2002).
6. **Moby Dick Nozzle:** This nozzle was developed in the nuclear industry as part of the French Nuclear Thermal Hydraulic code. The tests conducted during this research were done to study two phase critical flow conditions of such nozzles (Bestion, 1990). This nozzle is a mix of both circular and conical nozzle shape. The converging section is circular convex shape and the diverging section is linear.
7. **ASTAR Nozzle:** This nozzle was developed as part of the 'ASTAR Project' undertaken by European Union (Staedtke et al., 2005). It is a convergent - divergent nozzle, except its contour is more parabolic compared to a de Laval nozzle. The converging section of this nozzle is divided into two sections − the beginning of the nozzle is a circular convex shaped section, which is followed by a circular concave shaped section. The diverging section is a parabola.
8. **Deich Nozzle:** The Deich nozzle is also a de Laval nozzle, except its converging part is circular and its diverging part is parabolic. Another difference for this nozzle is its small divergent angle of 8° (Ashwood and Higgins, 1957).
9. **LJ Nozzle:** The LJ nozzle was created as part of this work, after 26 nozzle geometries had been tested on the single-phase horizontal facility. This geometry is very similar to one of the ASTAR nozzle geometries except it has a longer diverging section (40% longer divergent section compared to ASTAR nozzle 1).

Several physical geometrical parameters and testing variables can affect the performance of the nozzle, these include:

- Expansion ratio, which is the ratio of exit area to throat area
- Contraction ratio, which is the ratio of inlet area to throat area
- Throat length to throat diameter ratio
- Downstream to upstream pressure ratio
- Heat transfer
- Diverging Angle

3. Methodology

The nozzle design is an important component in this experimental research. Particular attention was paid to all nozzles design and construction. This included

https://doi.org/10.1016/j.heliyon.2019.e01273

calculating the appropriate nozzle throat size that would result in critical flow for the conditions available in the lab, creating an experimental matrix of different nozzle configurations, and generating the 3D drawings and 3D printed models. Finally, the horizontal nozzle test facility was designed and constructed.

The following conditions were available at the testing facility:

- Max. air flowrate = 74 cfm
- Max. air pressure = 80 psi

Based on these conditions, a throat size of 0.25 in. was chosen for all nozzle designs, to guarantee that the transition from critical to sub-critical flow can be determined during the experimental procedure.

In order to determine the effect of nozzle design parameters, such as converging angle, diverging angle and throat length, on nozzle performance, an experimental matrix was created that would include nozzle designs of varying parameters. In total, 49 configurations of nozzles were considered, but after initial testing, it was determined that certain nozzle shapes did not perform as well as others. Therefore, only 27 nozzles were experimentally tested. Table 1 presents the design parameters

Table 1. Design parameters and schematics for tested nozzles.

Nozzle type	Name	Nozzle number	Converging angle (°)	Diverging angle (°)	Convergent length (in)	Throat length (in)	Divergent length (in)
Conical	Group 1 nozzle	2	45	8	0.63	0.00	3.82
		3	45	12	0.63	0.00	2.92
		4	45	10	0.63	0.00	2.32
	Group 2 nozzle	1	45	8	0.63	0.50	4.45
		2	45	8	0.63	1.75	4.45
	Group 3 nozzle	1	84	8	0.56	0.00	4.44
Parabolic	Rao nozzle	1	45	30	0.70	0.00	1.87
		3	45	60	0.70	0.00	1.87
		4	45	90	0.70	0.00	2.01
		5	45	45	0.70	0.00	1.87
	Modified Rao nozzle	3	45	30	0.70	0.50	1.87
		7	45	60	0.70	0.50	1.87
		8	45	60	0.70	1.75	1.87
	Dual Bell nozzle	1	45	30/30	0.70	0.00	1.63
	Convex nozzle	1	30	30	3.16	0.40	1.87
	Concave nozzle	1	40	30	1.34	0.50	1.87
		2	40	60	1.34	0.50	1.87
	Moby Dick nozzle	1	45	7	1.17	0.50	0.59
		4	45	7	0.94	1.50	1.76
		2	45	12	0.94	0.50	0.59
	ASTAR nozzle	1	30	3	1.15	0.00	2.22
		2	30	10	1.15	0.00	2.37
		3	30	15	1.15	0.00	2.47
	Deich nozzle	1	36	8	1.67	0.00	2.08
		2	36	8	1.67	0.50	1.25
		3	36	8	1.67	1.75	1.25
	LJ nozzle	1	30	3	0.68	0.00	5.34

https://doi.org/10.1016/j.heliyon.2019.e01273

for the nozzles tested. Figs. 4 and 5 show the basic conical and parabolic nozzle geometries tested.

Basic profile designs of these nozzles were created using linear, parabolic and circular design equations. The 3D drawings that were required for 3D printing were created on Solidworks. A Stratasys Eden 260 VS 3D printer was used to create the physical nozzle models (Fig. 6). The material used for 3D printing was Vero White Resin. Pressure ports were included in the nozzle body design at different

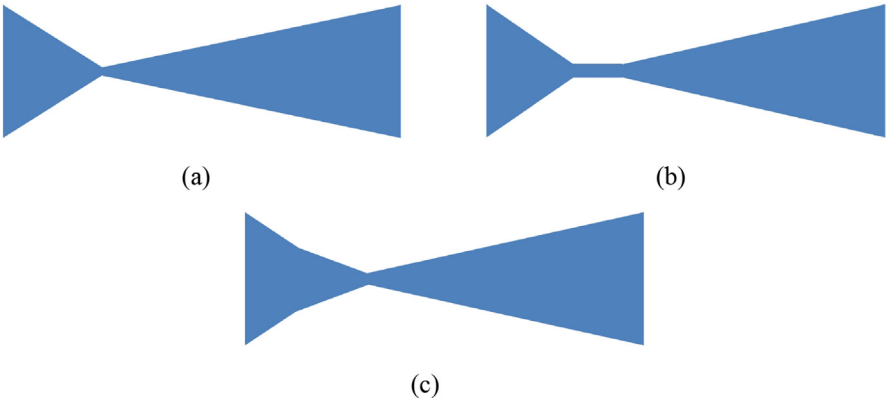

Fig. 4. Conical nozzles – (a) Group 1 nozzle, (b) Group 2 nozzle, (c) Group 3 nozzle.

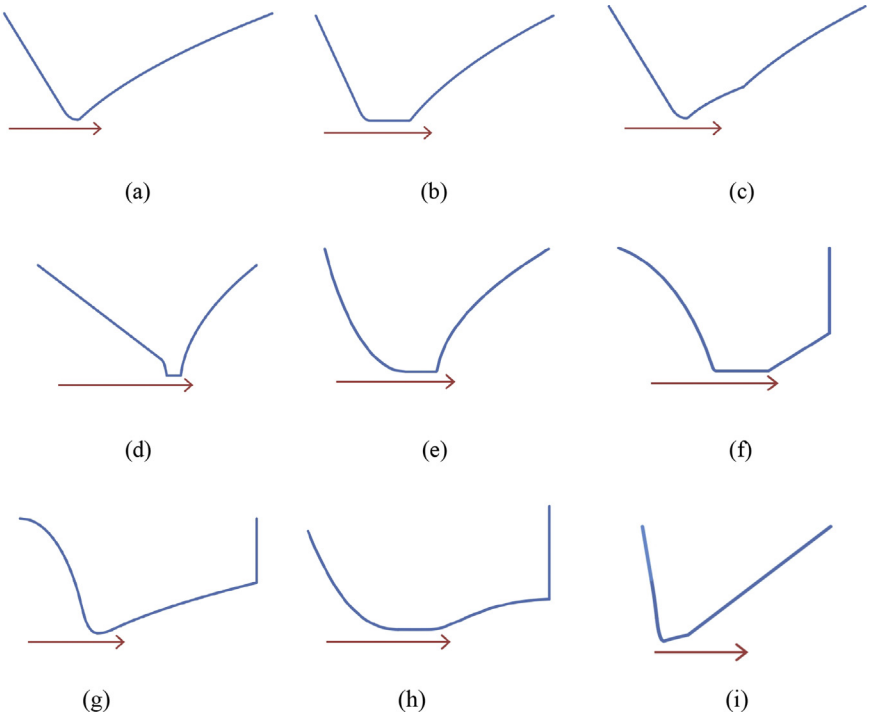

Fig. 5. Parabolic nozzles – (a) Rao nozzle, (b) Modified Rao nozzle, (c) Dual Bell nozzle, (d) Converging Convex nozzle, (e) Converging Concave nozzle, (f) Moby Dick nozzle, (g) ASTAR nozzle, (h) Deich nozzle, (i) LJ nozzle.

https://doi.org/10.1016/j.heliyon.2019.e01273

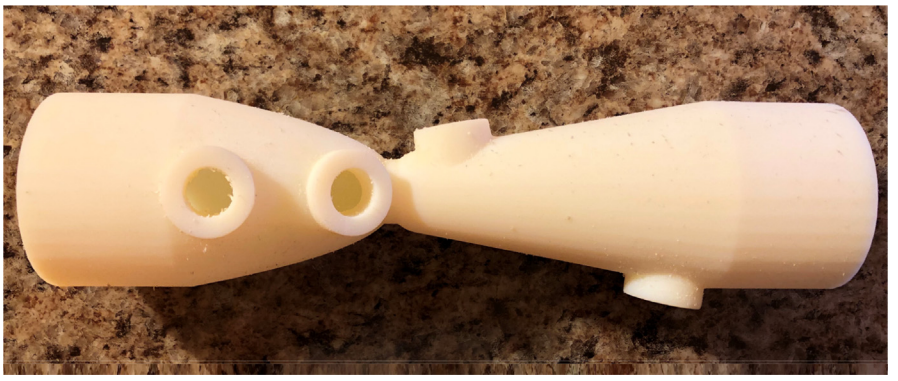

Fig. 6. 3D Printed model of a parabolic convex nozzle.

locations to record the pressure profile along the nozzle. Pressure transducers were tapped into these ports during the experimental phase. The number of ports for pressure transducers varied based on the space available on the nozzle body. The holes and threads were designed accordingly to fit the 0.25 in. pressure transducers and seal the holes. Both ends of the nozzle body consisted of sections that could be glued to 1.5 in. ID PVC unions.

4. Instrumentation

A horizontal facility was constructed to conduct single-phase nozzle flow testing (Fig. 7). The nozzle is installed on a 1.5 in. ID PVC pipe. Pressure and temperature transducers were installed along the pipelines. In total, there were 10 Rosemount pressure transducers (PT) and 3 Rosemount temperature transducers (TT) installed. One PT and TT was installed right after the point of gas injection to determine the pressure and temperature at which gas entered the system. Pressure and temperature transducers were installed upstream and downstream the nozzle to determine the pressure and temperature drop across the nozzle. At most, seven PT's were installed on the nozzle (depending on nozzle geometry). An air tank was installed after the air inlet to achieve additional volume of air in order to perform experiments at higher

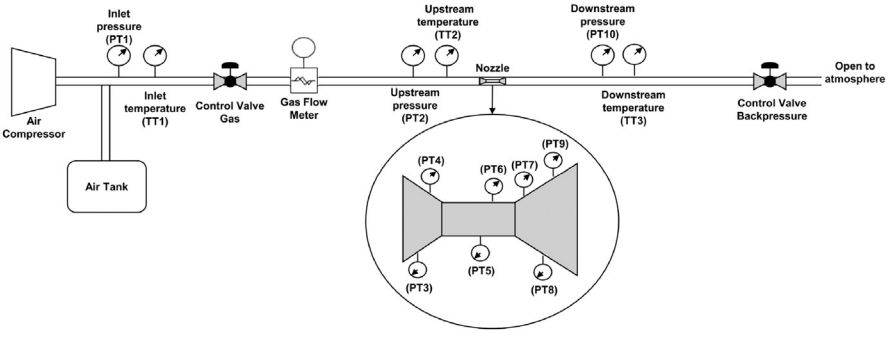

Fig. 7. Single-phase horizontal testing pipeline facility.

https://doi.org/10.1016/j.heliyon.2019.e01273

upstream pressures. A Vortex flowmeter was installed upstream of the nozzle in order to measure the gas flow rate. Two control valves were installed as part of the facility − one control valve was used to control the inlet gas pressure and the second control valve was installed at the end of the pipeline to control the back pressure. During a nozzle test, air is injected from a compressor into the pipe system. This air is vented out at the end of the pipeline facility to the atmosphere.

PTs, TTs, flowmeters and control valves were connected to an automation system (DeltaV system). This distributed control system was used to control the configuration of the valves and record data from the sensors connected to the system.

The following procedure was followed to perform the single-phase horizontal nozzle tests:

- Air was supplied to the inlet section of the pipeline and to the air tank.
- Both, gas control and the back-pressure valves were opened to 100%.
- Flow was allowed to stabilize by waiting 30 minutes.
- Next, the backpressure valve was closed by 10% every 5 minutes until the upstream gas flowrate started to decrease. Then, the backpressure valve was opened or closed until the critical point was determined (point where the upstream gas flowrate was no longer constant).
- Air supply was shut off and data was recorded from the DeltaV acquisition system.

5. Results & discussion

The upstream and downstream pressure, and upstream gas flow rate were measured to identify the transition between critical and subcritical flow and to determine the relative performance among the nozzles tested. Using these values, the downstream to upstream pressure ratio (P_d/P_u), and the pressure drop across the nozzle (P_u-P_d) were calculated. The critical pressure ratio was determined from a plot of upstream gas flowrate vs. upstream to downstream pressure ratio (Fig. 8). The last point recorded where the upstream gas flowrate was stable was chosen as the critical pressure ratio (shown by a black arrow mark on Fig. 8). The flow is critical for lower pressure ratios and is sub-critical for larger pressure ratios. Table 2 shows the pressure drop, critical pressure ratio, upstream pressure and upstream gas flow rate for all nozzles tested at the critical/subcritical flow transition.

The relative nozzle performance was evaluated based on two performance measures: the critical pressure ratio and the nozzle pressure drop. Two separate rankings are presented in Table 3 based on these two parameters, one for decreasing pressure ratio and other for increasing pressure drop. By doing so, it was observed that nozzles that had a high critical pressure ratio did not necessarily have the least pressure drop.

https://doi.org/10.1016/j.heliyon.2019.e01273

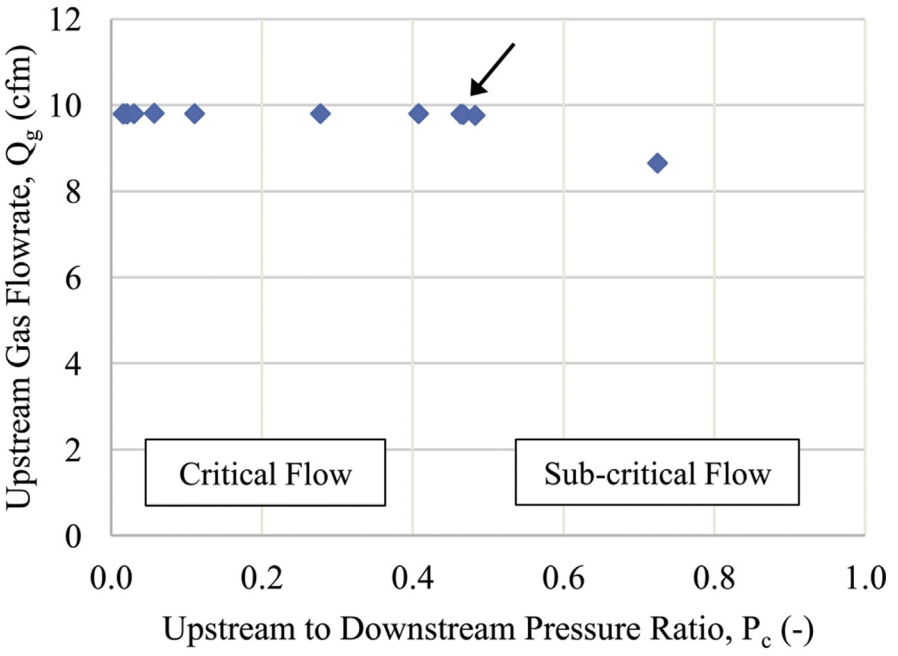

Fig. 8. Identifying the critical pressure ratio – point of transition from critical to sub-critical flow.

Table 2. Single-phase horizontal flow experimental results.

Nozzle			Pressure drop, dP (psi)	Critical pressure ratio, P_c (-)	Upstream pressure, P_u (psi)	Upstream gas flowrate, $Q_{u,g}$ (cfm)
Conical	Group 1	Nozzle 2	13.1	0.30	18.7	12.9
		Nozzle 3	15.6	0.24	20.6	12.6
		Nozzle 4	15.4	0.36	24.1	12.2
	Group 2	Nozzle 1	15.6	0.34	23.6	12.4
		Nozzle 3	18.4	0.45	30.0	9.8
	Group 3	Nozzle 1	9.3	0.57	21.8	13.0
Parabolic	Rao Bell	Nozzle 1	11.6	0.18	15.1	16.6
		Nozzle 3	14.4	0.33	21.6	12.7
		Nozzle 4	12.8	0.31	16.6	13.0
		Nozzle 5	13.6	0.44	24.3	12.3
	Modified Rao Bell	Nozzle 3	17.4	0.21	22.0	11.9
		Nozzle 7	20.0	0.24	26.3	11.3
		Nozzle 8	18.3	0.44	24.3	10.2
	Dual Bell	Nozzle 1	12.7	0.43	22.4	12.7
	Convex Bell	Nozzle 1	15.1	0.41	25.6	11.8
	Concave Bell	Nozzle 1	21.0	0.22	26.2	11.4
		Nozzle 2	16.4	0.28	22.9	11.4
	ASTAR	Nozzle 1	6.0	0.75	23.8	12.3
		Nozzle 2	9.8	0.58	21.2	12.9
		Nozzle 3	10.2	0.48	19.6	12.7
	Moby Dick	Nozzle 1	11.3	0.49	21.9	11.9
		Nozzle 2	14.5	0.34	22.0	11.7
		Nozzle 4	13.4	0.50	26.3	10.1
	Deich	Nozzle 1	12.3	0.53	25.9	11.5
		Nozzle 2	12.6	0.54	27.5	10.9
		Nozzle 3	14.9	0.56	33.8	9.2
	LJ	Nozzle 1	7.9	0.65	22.2	12.0

https://doi.org/10.1016/j.heliyon.2019.e01273

Table 3. Ranking of nozzle performance based on both critical pressure ratio and pressure drop.

Nozzle			Rank – pressure drop	Rank – critical pressure ratio
Conical	Group 1	Nozzle 2	12	21
		Nozzle 3	20	23
		Nozzle 4	19	16
	Group 2	Nozzle 1	21	18
		Nozzle 3	25	11
	Group 3	Nozzle 1	3	4
Parabolic	Rao Bell	Nozzle 1	7	27
		Nozzle 3	15	19
		Nozzle 4	11	20
		Nozzle 5	14	12
	Modified Rao Bell	Nozzle 3	23	26
		Nozzle 7	26	24
		Nozzle 8	24	13
	Dual Bell	Nozzle 1	10	14
	Convex Bell	Nozzle 1	18	15
	Concave Bell	Nozzle 1	27	25
		Nozzle 2	22	22
	ASTAR	**Nozzle 1**	**1**	**1**
		Nozzle 2	**4**	**3**
		Nozzle 3	**5**	**10**
	Moby Dick	**Nozzle 1**	**6**	**9**
		Nozzle 2	16	17
		Nozzle 4	13	8
	Deich	**Nozzle 1**	**8**	**7**
		Nozzle 2	**9**	**6**
		Nozzle 3	17	5
	LJ	**Nozzle 1**	**2**	**2**

Bold values in Table 3 indicate group of nozzles that showed best performance in terms of critical pressure ratio and pressure drop, as mentioned in the text.

From Table 3, it can be noted that four nozzle groups performed best when both criteria are taken into consideration – ASTAR, Deich, Moby Dick and LJ. Nozzles in these geometric configurations are considered optimal geometries. From these optimal geometries, the most optimum was the ASTAR Nozzle 1, it had the highest critical pressure ratio and the lowest pressure drop.

In order to understand why some nozzle geometries performed better than others, the pressure readings recorded at different locations of the nozzle were studied. Because there were different number of PTs on each nozzle, to analyze the data consistently, the nozzle area was divided into four regions and single pressure reading from each region were chosen. The first region includes the area from pipe to the convergent section, the second region includes the area from convergent section to throat to beginning of divergent section, the third region includes the area from beginning of divergent section to the end of divergent section, and the fourth region includes the area from the end of divergent section to the pipe area. Also, since the upstream pressure varied slightly in the experiments, the pressures at each region were normalized to the upstream pressure (i.e., ratio of region pressure to upstream pressure) for analysis.

https://doi.org/10.1016/j.heliyon.2019.e01273

Fig. 9 shows how the normalized pressure (pressure ratio) at each region changes across the nozzle. From this figure, it can be noted that the region that has the most impact on the pressure drop behavior is region 2, which includes the throat. Therefore, the shape of the area right before the throat, the throat and shape of the area right after the throat play a significant role in determining the pressure drop across the nozzle.

Figs. 10 and 11 show the pressure ratio profile as it changes with flow through the nozzle for optimal geometries and non-optimal geometries, respectively. There are two main reasons some geometries performed better than the others − 1) magnitude of pressure drop in region 2, 2) pressure recovery in region 3 and region 4. A stark difference can be observed in optimal and non-optimal geometries if these reasons are considered. In case of optimal geometries, the pressure drop in region 2 is lower than in non-optimal geometries. The range of pressure ratio at region 2 (right after the throat) for optimal geometries is from 0.40 to 0.58. In case of non-optimal geometries, the range is 0.15−0.39. Along with this, it can also be observed that the pressure generally recovers in case of optimal geometries. This results in a lower overall

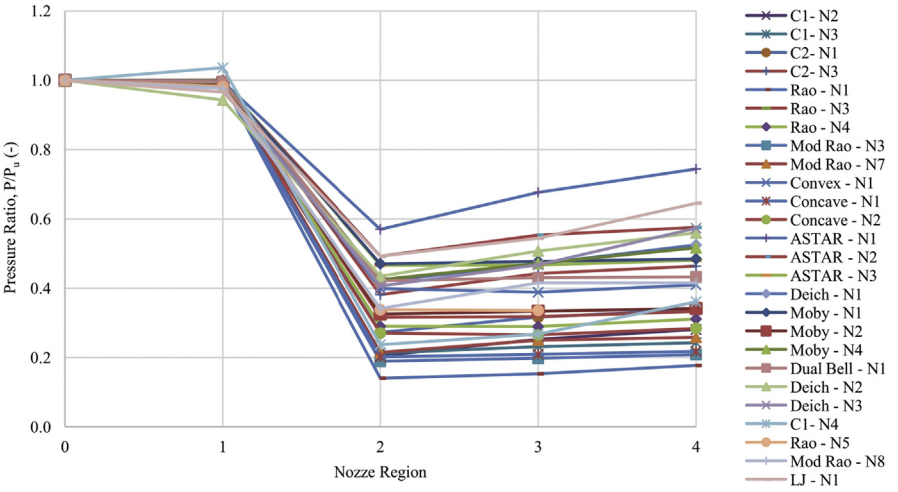

Fig. 9. Pressure drop ratio across nozzle for single-phase horizontal flow tests.

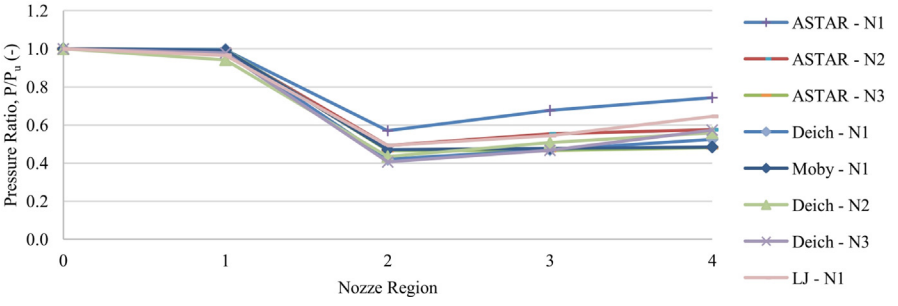

Fig. 10. Change in pressure drop ratio across nozzle for optimal geometries.

https://doi.org/10.1016/j.heliyon.2019.e01273

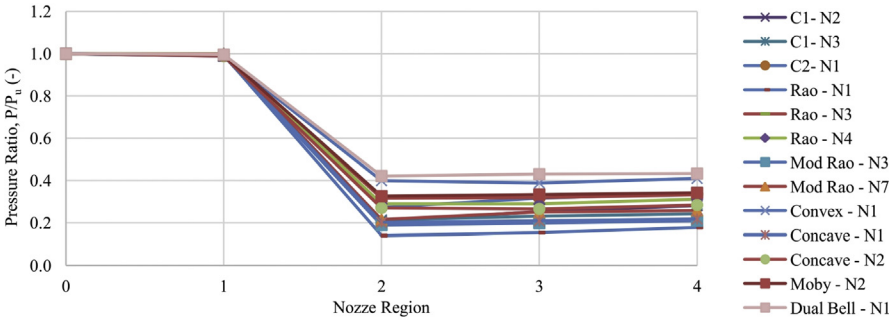

Fig. 11. Change in pressure drop ratio across nozzle for non-optimal geometries.

pressure drop across the nozzle and a higher critical point. For the non-optimal nozzles, the velocity is still high in regions 3 and 4 and as a result, the pressure recovery does not occur. This results in a higher pressure drop across the nozzle and a lower critical point.

Based on results obtained, the effect of increasing diverging angles, elongating the throat lengths and increasing overall length of the nozzle can be observed among different nozzle groups. The effect of these parameters will be discussed below for the basic conical and parabolic nozzle shapes as the sub groups of these nozzles followed similar patterns.

By analyzing data from Conical group 1 nozzles, the effect of changing diverging angle in a conical nozzle was determined. Three different nozzles with diverging angles of 8°, 10° and 12° were tested. Fig. 12 shows the results from these tests. It can be noted that the nozzle with the highest critical pressure ratio is the one with a diverging angle of 10°, followed by 8° and 12°. In general, a loss on performance is observed as the diverging angle is increased. Similar trend can be observed in the Moby Dick nozzles, where the diverging section is conical.

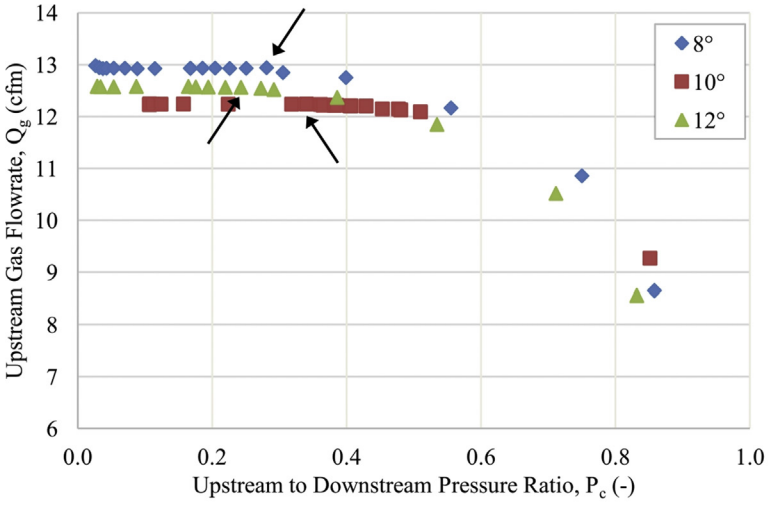

Fig. 12. Effect of varying diverging angles on nozzle performance for conical shaped nozzles.

https://doi.org/10.1016/j.heliyon.2019.e01273

By analyzing data from Conical group 2 and group 1 nozzles, the effect of elongated throat lengths in a conical nozzle can be determined. Three different nozzles with throat lengths of 0 in., 0.5 in. and 1.5 in. and the same diverging angle of 8° were tested. Fig. 13 shows the results from this test. A longer elongated throat resulted in a higher critical pressure ratio. However, since the velocity of air is higher for a longer length in nozzles with larger elongated throats, the frictional pressure drop across the nozzle is higher. This results in a higher pressure drop across the nozzle. Therefore, a longer elongated throat is not ideal for optimal performance. Similar trends can be observed in Moby Dick nozzles.

By analyzing data from Rao nozzles, the effect of changing diverging angles in a parabolic nozzle with no elongated throat can be determined. Three different nozzles with diverging angles of 45°, 60° and 90° were tested. Fig. 14 shows the results from these tests. It can be noted that similar to conical nozzles, the nozzle with the smallest diverging angle resulted in the highest critical pressure ratio. A loss of nozzle performance is observed as the diverging angle is increased. Similar trends can be observed in ASTAR nozzles. For parabolic nozzles with an elongated throat, nozzle performance increases for a higher diverging angle. Such trends can be observed in Modified Rao and Concave Bell nozzles.

By analyzing data from Modified Rao and Rao nozzles, the effect of different elongated throat lengths in a parabolic nozzle can be determined. Two different nozzles with throat lengths of 0 in. and 1.5 in. and a diverging angle of 60° were tested. Fig. 15 shows the results from these tests. Nozzle performance in terms of critical pressure ratio increases as length of throat increases, but similar to conical nozzles,

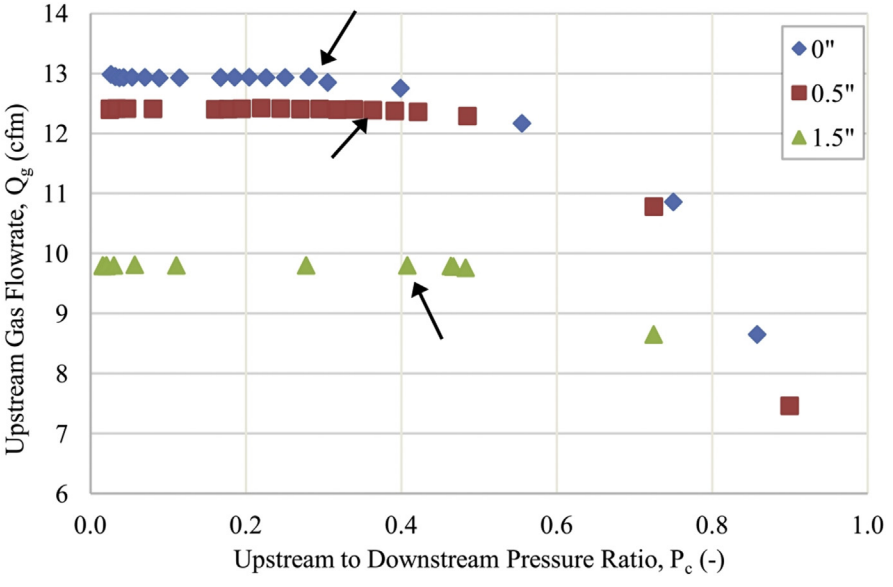

Fig. 13. Effect of varying throat lengths on nozzle performance for conical shaped nozzles.

https://doi.org/10.1016/j.heliyon.2019.e01273

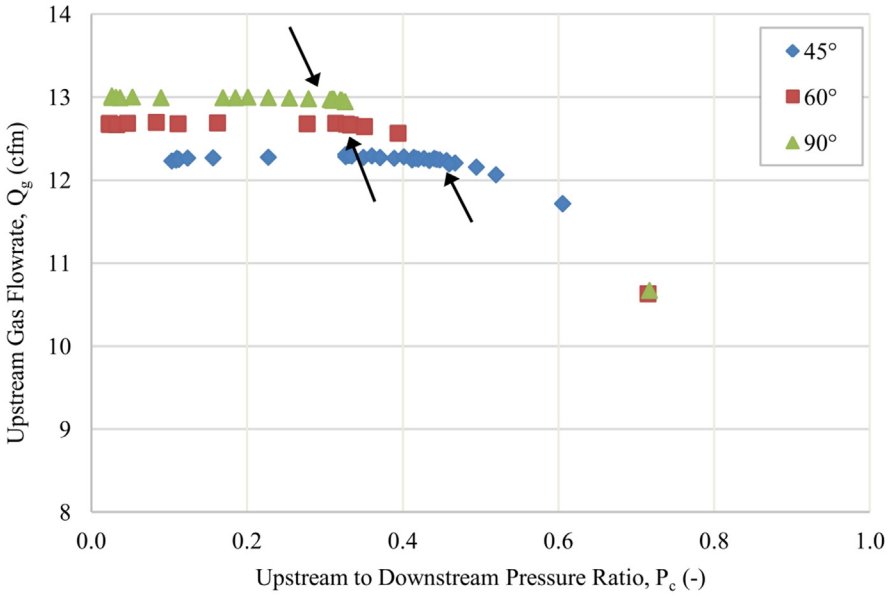

Fig. 14. Effect of varying diverging angles on nozzle performance for parabolic shaped nozzles.

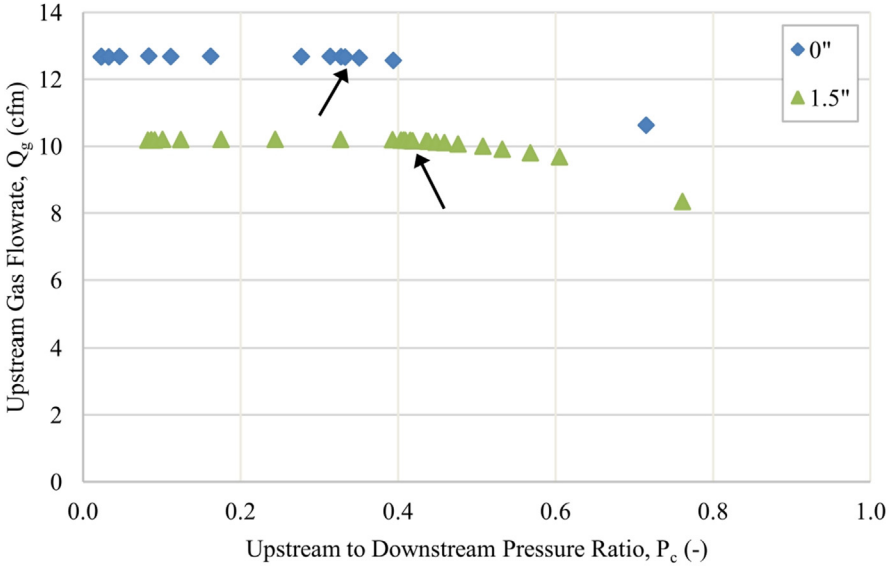

Fig. 15. Effect of varying throat lengths on nozzle performance for parabolic shaped nozzles.

the pressure drop across the nozzle increases as well with an increase in throat length. Similar trend can be observed in the three Deich nozzles, however the effect of throat length is not too profound in this case as the critical pressure ratio for all three nozzles are very close to each other.

By analyzing the results from ASTAR nozzle 1 and LJ nozzle 1, the effect of total nozzle length on nozzle performance can be determined. Both have similar geometry right before and right after the throat, except LJ nozzle is longer in length compared

https://doi.org/10.1016/j.heliyon.2019.e01273

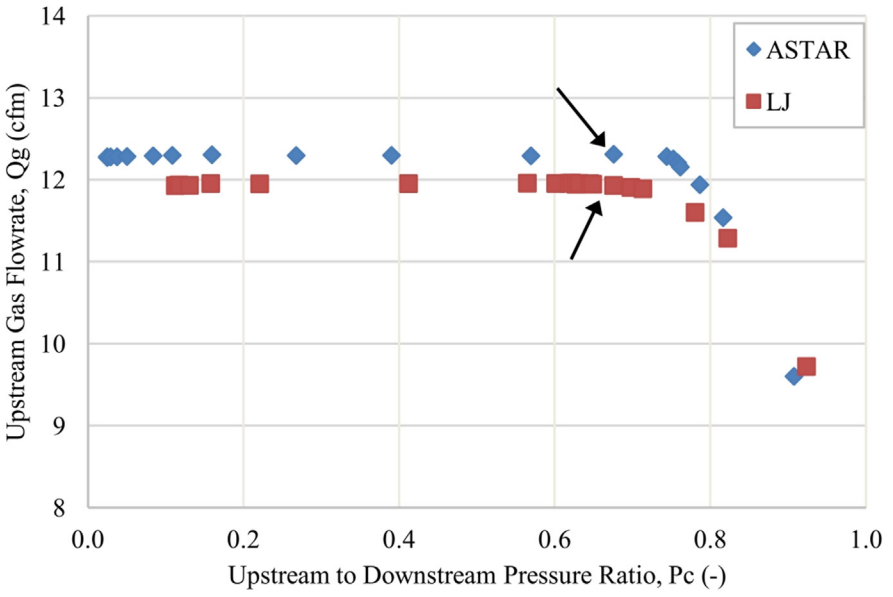

Fig. 16. Effect on nozzle length on nozzle performance.

to ASTAR nozzle. Fig. 16 shows the results from this test. It can be observed that the critical pressure ratio for both nozzles is very similar. The only difference in performance is that the LJ nozzle has a slightly higher pressure drop across the nozzle.

The presence of pressure transducers along the nozzle body has an effect on the nozzle performance. As the fluid moves through the nozzle, the transducers make the flow more turbulent and this results in a higher pressure drop across the nozzle and a lower critical pressure ratio. In order to determine the effect of this turbulence, three nozzles were tested without pressure transducers mounted on them. The critical pressure ratio on average lowered by 0.06 and the pressure drop across the nozzle increased by 2.5 psi due to the presence of pressure transducers.

6. Conclusions

Single-phase compressible flow experiments were performed to determine the optimal nozzle geometry that maximizes critical pressure ratio and minimizes pressure drop across the nozzle. By testing 27 different nozzle geometries, the data obtained was analyzed to determine the effect of nozzle geometrical parameters on nozzle performance. From the experimental study, the following conclusions can be made:

- Nozzle geometry does have a significant impact of nozzle performance. Effect of single-phase air flow through a nozzle revealed the effect of different nozzle parameters on nozzle performance. A lower diverging angle and no elongated throat gave the best critical pressure ratio and a low pressure drop. The length

https://doi.org/10.1016/j.heliyon.2019.e01273

of the nozzle did not have as much of an effect on the performance as the shape of the nozzle right before and after the throat. And the shape of diverging section is important to promote pressure recovery.

- Based on the results, ASTAR nozzle configuration was the most optimal. In particular, ASTAR nozzle 1 geometry performed the best as it had the highest critical pressure ratio valve and the lowest pressure drop. This geometry had a diverging angle of 3°, a parabolic diverging section, no elongated throat and a convex and concave converging section.

Declarations

Author contribution statement

Jagmit Singh: Performed the experiments; analyzed and interpreted the data; wrote the paper.

Luis Zerpa: Conceived and designed the experiments; analyzed and interpreted the data; wrote the paper.

Benjamin Partington, Jose Gamboa: Conceived and designed the experiments; Analyzed and interpreted the data.

Funding statement

This work was supported by Chevron ETC.

Competing interest statement

The authors declare no conflict of interest.

Additional information

No additional information is available for this paper.

Acknowledgements

The authors would like to greatly acknowledge the support from Chevron for providing valuable technical support throughout the entire project.

References

Almeida, A.R., 2015. some design aspects for venturi gas lift valves. SPE Prod. Oper. 30.

https://doi.org/10.1016/j.heliyon.2019.e01273

Ashwood, P.F., Higgins, D.G., 1957. The Influence of Design Pressure Ratio and Divergence Angle on the Thrust of Convergent-Divergent Propelling Nozzles. Aeronautical Research Council. C.P. No. 325.

Barber, R.E., Schultheiss, M.J., 1967. Effect of nozzle geometry on off-design performance of partial admission impulse turbines. Off. Naval Res. 49–52. PR010-04-01.

Bestion, D., 1990. The physical closure laws in the CATHARE code. Nucl. Eng. Des. 124, 229–245.

Clarke, C.J., Carswell, B., 2007. Principles of Astrophysical Fluid Dynamics. Cambridge University Press, Cambridge, UK.

Elliot, D.G., Weinber, E., 1968. Acceleration of Liquids in Two-Phase Nozzles. Jet Propulsion Lab, Pasadena, CA, pp. 16–34.

Kulhanek, S.L., 2012. Design, Analysis, and Simulation of Rocket Propulsion System. MS Thesis. University of Kansas, Lawrence, Kansas.

Nürnberger-Genin, C., Stark, R., 2009. Flow transition in dual bell nozzles. Shock Waves 19, 265–270.

Östlund, J., 2002. Flow Processes in Rocket Engine Nozzles with Focus on Flow Separation and Side-loads. MS Thesis. Royal Institute of Technology, Stockholm.

Park, K.A., Choi, Y.M., Choi, H.M., March, 2001. The evaluation of critical pressure ratios of sonic nozzles at low reynolds numbers. Flow Meas. Instrum. 12, 37–41.

Popov, S.A., 2002. Liquid-Gas Ejector with an Improved Liquid Nozzle and Variants. United States Patent Application Publication, US20020079384A1.

Raiano, M., 2013. Rocket Engines, 21 November 2013. http://www.aerospacengineering.net/?p=1241. (Accessed 7 March 2018).

Staedtke, H., Franchello, G., Worth, B., et al., 2005. Advanced three-dimensional two-phase flow simulation tools for application to reactor safety (ASTAR). Nucl. Eng. Des. 235, 379–400.

Sutton, G., Biblarz, O., 2001. Rocket Propulsion Elements. Wiley.

https://doi.org/10.1016/j.heliyon.2019.e01273